Journal of Alloys and Compounds 509 (2011) 1249–1254

Contents lists available at ScienceDirect

Journal of Alloys and Compounds

journal homepage: www.elsevier.com/locate/jallcom

Composition dependence of magnetic properties of directly quenched Nd–Fe–Ti–Zr–B bulk magnets

H.W. Chang[a,*], Y.T. Cheng[b], C.C. Hsieh[b], W.C. Chang[b,*], A.C. Sun[c]

[a] Department of Physics, Tunghai University, Taichung 407, Taiwan, ROC
[b] Department of Physics, National Chung Cheng University, Chia-Yi 621, Taiwan, ROC
[c] Department of Chemical Engineering and Materials Science, Yuan Ze University, Chung-Li 320, Taiwan, Taiwan, ROC

ARTICLE INFO

Article history:
Received 4 August 2010
Received in revised form
30 September 2010
Accepted 30 September 2010
Available online 8 October 2010

PACS:
74.25.Ha
75.50.Vv
75.50.Ww

Keywords:
Magnetic intermetallics
Magnetic properties
Copper mold casting

ABSTRACT

Magnetic properties, phase evolution, and microstructure of directly quenched $Nd_yFe_{97-y-z}Ti_{3-x}Zr_xB_z$ (x = 0–3; y = 7–10; z = 14–19) bulk magnets of 0.9 mm in diameter have been investigated. Proper Zr substitution for Ti and appropriate Nd and B contents modify the magnetic phases constitution and refine the grain size from 200–250 nm to 50–100 nm. Consequently, the magnetic properties of the rods are enhanced remarkably from ${}_iH_c$ = 6.2 kOe and $(BH)_{max}$ = 5.6 MGOe for Zr-free rods to ${}_iH_c$ = 6.7–13.5 kOe and $(BH)_{max}$ = 6.7–8.2 MGOe for Zr-substituted $Nd_yFe_{97-y-z}Ti_{3-x}Zr_xB_z$ rods (x = 0.5–2; y = 8–10; z = 14–16). The optimum magnetic properties of B_r = 6.6 kG, ${}_iH_c$ = 9.6 kOe and $(BH)_{max}$ = 8.2 MGOe were achieved for $Nd_{9.5}Fe_{72.5}Ti_{2.5}Zr_{0.5}B_{15}$ alloy.

1. Introduction

In the R–Fe–B system, two types of nanocomposites, $R_2Fe_{14}B/\alpha$-Fe and $R_2Fe_{14}B/Fe_3B$, have been widely developed via melt spinning for bonded magnet applications, because their remanence B_r and maximum energy product $(BH)_{max}$ can be effectively enhanced by exchange coupling between magnetically soft and hard phases [1–8]. Traditionally, the bonded magnets have been produced from molding the powders, obtained by combining the crushing melt spun ribbons, fabricated at an optimal quenching velocity and followed by post annealing with proper temperature, with a polymer binder. The main disadvantages of the traditional method include multifarious manufacturing processes and the dilution of magnetic properties by nonmagnetic polymer.

To overcome these disadvantages, a new group of R–Fe–M–B (R = Pr, Pr + Dy, Nd + Dy; M = Co, Cu, Mo, Nb, Ti, V, and Zr) bulk metallic glasses have been developed by copper mold casting method, and then followed by one-step heat treatment to optimize the permanent magnetic properties [9–13]. The compositions with the extremely high B content, such as $R_{3-4.5}Fe_{bal.}M_xB_{20}$ (R = Pr, Pr + Dy, Nd + Dy; M = Co, Cu, Mo, Nb, Ti, V, and Zr), were adopted in order to produce bulk amorphous precursor in rod form with 0.5–0.6 mm in diameter at first, and then they were annealed at 600–700 °C for 10–30 min [9–13]. Although higher $(BH)_{max}$ of 7.3–12.0 MGOe can be attained, the intrinsic coercivity (${}_iH_c$) is too low (<4 kOe), resulting from the existence of considerable amount of the magnetically soft phases α-Fe or Fe_3B, to suit for high temperature or thin magnets applications.

Furthermore, to improve the coercivity of the bulk magnets, Zhang et al. [14] used $Nd_{9.6}Fe_{bal.}Nb_4B_{22.08}$ as the base alloy and it showed a high coercivity of 13.8 kOe but a relatively low $(BH)_{max}$ (~4 MGOe). Additionally, to make sheet specimens with larger area size, Tan et al. [15] demonstrated $Nd_5Y_4Fe_{68}Zr_2B_{21}$ bulk magnets with the size of 0.8 mm × 10 mm × 50 mm, and nevertheless, the ordinary magnetic properties of ${}_iH_c$ = 4.8 kOe and $(BH)_{max}$ = 5.4 MGOe were obtained. Meanwhile, in our previous studies [16–18], in order to further simplify manufacturing process for making isotropic magnet, by composition modification, directly quenched $Pr_{9.5}Fe_{71.5}Nb_4B_{15}$ and $Nd_{9.5}Fe_{72.5}Ti_3B_{15}$ bulk magnets, 0.7 mm in diameter, with the optimal magnetic properties of B_r = 5.7 kG, ${}_iH_c$ = 16.2 kOe and $(BH)_{max}$ = 7.1 MGOe, and B_r = 6.5 kG, ${}_iH_c$ = 10.3 kOe and $(BH)_{max}$ = 8.7 MGOe, respectively, have been developed.

In this study, to further increase the size of the bulk magnet and to maintain the attractive magnetic properties, Zr is selected

* Corresponding authors. Tel.: +886 4 23594778; fax: +886 4 23594778.
E-mail addresses: wei0208@gmail.com (H.W. Chang), phywcc@ccu.edu.tw (W.C. Chang).

0925-8388/$ – see front matter © 2010 Elsevier B.V. All rights reserved.
doi:10.1016/j.jallcom.2010.09.204

to replace Ti in $Nd_{9.5}Fe_{72.5}Ti_3B_{15}$ alloy based on Inoue's empirical rules [19] and our previous study [17]. We report on the effects of Zr substitution for Ti and also of Nd and B contents on the magnetic properties, phase evolution, and microstructure of directly quenched $Nd_yFe_{97-y-z}Ti_{3-x}Zr_xB_z$ (x = 0–3; y = 7–10; z = 14–19) magnets with a 0.9 mm in diameter and a length of 15 mm.

2. Experimental

Alloy ingots with nominal compositions of $Nd_yFe_{97-y-z}Ti_{3-x}Zr_xB_z$ (x = 0–3; y = 7–10; z = 14–19) were prepared by arc melting mixtures of pure Nd, Fe, M metal and pure B crystal in an argon atmosphere. 5% excess Nd was adopted to compensate the loss of Nd during processing. These magnetic rods with cylindrical shape of a diameter of 0.9 mm and 15 mm in length were obtained by injection casting into a copper mold. The crystalline structures were identified by X-ray powder diffraction (XRD) with Cu-K_α radiation. The Curie temperatures of magnetic phases were determined by a thermal gravimetric analyzer (TGA) with an externally applied magnetic field (conventionally referred as "TMA"), under a heating rate of 20 °C/min. The macroscopic morphology of the cross section of rods was studied using a scanning electron microscopy (SEM), while the microstructure was directly observed by a transmission electron microscopy (TEM). The magnetic properties of the rods at room temperature were measured by a vibrating sample magnetometer (VSM). All samples were magnetized by a 50 kOe peak pulse field prior to magnetic measurement.

3. Results and discussion

In our previous studies [17,18], magnetic properties of B_r = 6.5 kG, $_iH_c$ = 10.3 kOe, and $(BH)_{max}$ = 8.7 MGOe were obtained for directly quenched $Nd_{9.5}Fe_{72.5}Ti_3B_{15}$ magnets with a diameter of 0.7 mm and a length of 15 mm. However, increasing the diameter of the magnet to 0.9 mm degraded the magnetic properties to B_r = 6.0 kG, $_iH_c$ = 6.2 kOe, and $(BH)_{max}$ = 5.6 MGOe, because the grain size becomes coarser and the size distribution turns out to be inhomogeneous in the magnet due to its slower cooling rate. To improve the permanent magnetic properties of the directly quenched cylindrical magnet with a larger diameter of 0.9 mm, effect of Zr substitution for Ti on the magnetic properties and phase evolution of directly quenched $Nd_{9.5}Fe_{72.5}Ti_{3-x}Zr_xB_{15}$ (x = 0–3) magnets have been studied. Fig. 1 shows the second quadrant demagnetization curves of $Nd_{9.5}Fe_{72.5}Ti_{3-x}Zr_xB_{15}$ alloys. Obviously, proper Zr substitution for Ti in $Nd_{9.5}Fe_{72.5}Ti_{3-x}M_xB_{15}$ magnets can improve $(BH)_{max}$ and $_iH_c$ simultaneously. When the Zr content x is increased, B_r and $(BH)_{max}$ are increased up to maximum

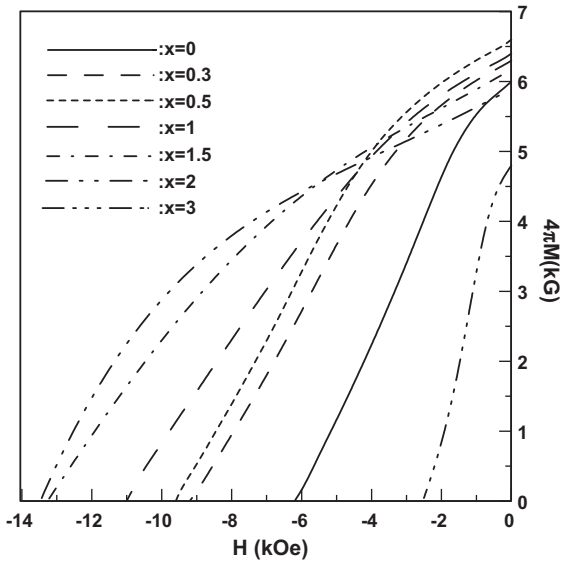

Fig. 1. Demagnetization curves of directly quenched $Nd_{9.5}Fe_{72.5}Ti_{3-x}Zr_xB_{15}$ (x = 0–3) magnets with a diameter of 0.9 mm.

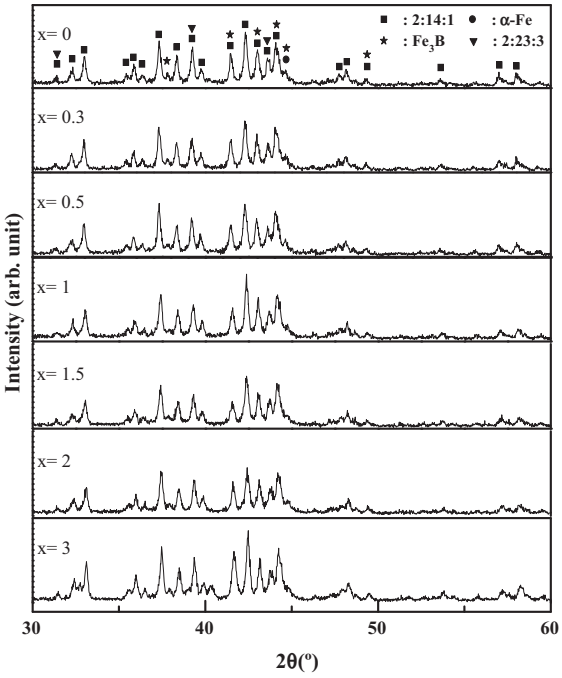

Fig. 2. XRD patterns of directly quenched $Nd_{9.5}Fe_{72.5}Ti_{3-x}Zr_xB_{15}$ (x = 0–3) magnets.

respective values of 6.6 kG and 8.2 MGOe for x = 0.5, then slightly decreased to 6.4–5.9 kG and 7.8–6.9 MGOe for x = 1–2 and rapidly reduced to 4.8 kG and 2.4 MGOe respectively for x = 3; on the other hand, $_iH_c$ is increasing from 6.2 kOe for x = 0–13.5 kOe for x = 2 at first, and then drastically reduced to 2.5 kOe for x = 3. Thus, the optimal magnetic properties are achieved for $Nd_{9.5}Fe_{72.5}Ti_{2.5}Zr_{0.5}B_{15}$ magnets.

The above results reflect that substitution of suitable amount of Zr for Ti in bulk $Nd_{9.5}Fe_{72.5}Ti_{3-x}Zr_xB_{15}$ magnets is effective in enhancing both $_iH_c$ and $(BH)_{max}$, and thus, it is of interest to understand why appropriate Zr substitution for Ti can improve the magnetic properties through phase identification and microstructure studies. Fig. 2 shows X-ray diffraction patterns of directly quenched $Nd_{9.5}Fe_{72.5}Ti_{2.5}Zr_{0.5}B_{15}$ bulk magnets. For all the samples, almost all diffraction peaks of 2:14:1 phase are overlapped with those of 2:23:3, Fe_3B, α-Fe, or other existing phases to complicate the phase identification. Nevertheless, it is seen that the full width at half of the maximum (FWHM) for diffraction peaks slightly become broadened with Zr substitution, suggesting that the crystalline size is refined with proper Zr substitution for Ti, except for $Nd_{9.5}Fe_{72.5}Zr_3B_{15}$.

To understand the magnetic phases constitution in directly quenched $Nd_{9.5}Fe_{72.5}Ti_{3-x}Zr_xB_{15}$ magnets, TMA technique was used. Fig. 3 presents TMA scans of directly quenched $Nd_{9.5}Fe_{72.5}Ti_{3-x}Zr_xB_{15}$ magnets. For Zr-free $Nd_{9.5}Fe_{72.5}Ti_3B_{15}$ magnet, the large volume fraction of magnetically hard 2:14:1 phase is found to coexist with small amounts of magnetically soft Fe_3B and α-Fe phases. As Zr is substituted for Ti, the amount of α-Fe phase slightly increases for x = 0.3–1.5. This might be one of the reasons why the remanent magnetization of these magnets is larger than that for x = 0. However, as Zr content x increases to 3, the significant decrease of the volume fraction of 2:14:1 phase accompanies the increase of the amount of α-Fe phase, leading to the drastic decrease of the magnetic characteristics. This implies that more Zr substitution for Ti may make the 2:14:1 phase more unstable, which is in accordance with the result of our previous study [17]. Besides, from Fig. 3, it can also be seen that the Curie temperature (T_C) of 2:14:1 phase is reduced with Zr substitution

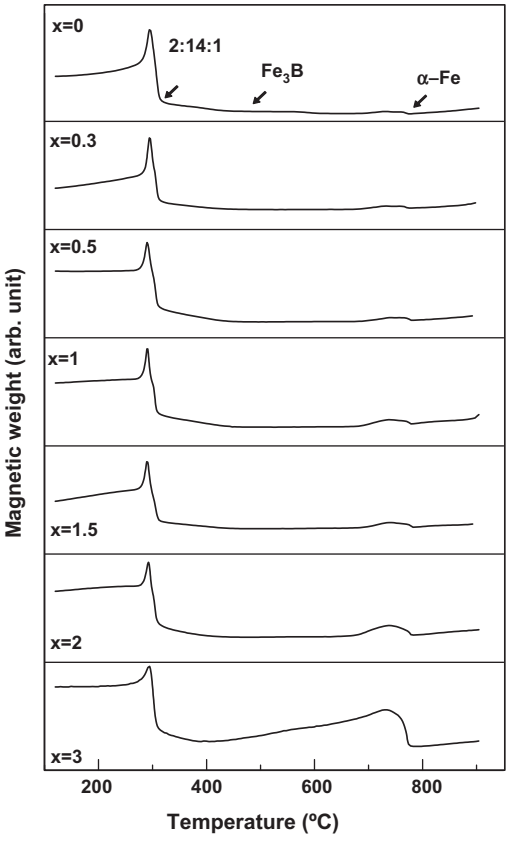

Fig. 3. TMA scans of directly quenched $Nd_{9.5}Fe_{72.5}Ti_{3-x}Zr_xB_{15}$ (x = 0–3) magnets.

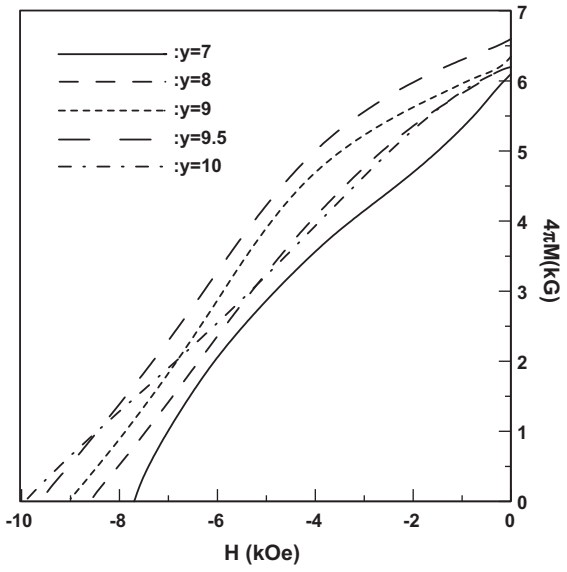

Fig. 4. Demagnetization curves of directly quenched $Nd_yFe_{82-y}Ti_{2.5}Zr_{0.5}B_{15}$ bulk magnets.

for Ti, from 315 °C for x = 0 to 306 °C for x = 3, revealing that part of Zr element tends to enter into the crystal structure by forming (Nd, Zr)$_2$Fe$_{14}$B phase. This result is in agreement with that reported by Chen [20]. Besides, Jurczyk reported that introducing proper amount of Zr in 2:14:1 phase may increase the anisotropy field of the alloy [21], and accordingly $_iH_c$ is remarkably increased with Zr substitution.

Furthermore, the effect of Nd content on the magnetic properties and phase evolution of directly quenched $Nd_yFe_{82-y}Ti_{2.5}Zr_{0.5}B_{15}$ (y = 7–10) magnets was also studied. Fig. 4 shows their second quadrant demagnetization curves. Clearly, with the decrease of Nd content y, B_r slightly increases from 6.1 kG for y = 10 to 6.6 kG for y = 9.5 at first, and then decreases to 6.1 kG for y = 7. On the contrary, $_iH_c$ decreases monotonously from 10 kOe for y = 10 to 7.7 kOe for y = 8. Besides, the squareness (SQ) of demagnetization curve with shoulder phenomenon is found for y = 7. Therefore, with the decrease of Nd content, $(BH)_{max}$ slightly increases from 6.7 MGOe for y = 10 to reach the maximum value of 8.2 MGOe for y = 9.5 at first, and then decreases to 4.5 MGOe for y = 7. It is worthy to note that the directly quenched $Nd_yFe_{82-y}Ti_{2.5}Zr_{0.5}B_{15}$ (y = 8–10) rods with a diameter of 0.9 mm could exhibit high coercivity and large energy product simultaneously.

Fig. 5 presents TMA scans of $Nd_yFe_{82-y}Ti_{2.5}Zr_{0.5}B_{15}$ bulk magnets. It is found that the large volume fraction of magnetically hard 2:14:1 phase coexists with minor amounts of soft Fe$_3$B and α-Fe phase. In addition, the volume fraction of 2:14:1 phase decreases with decreasing Nd content, giving rise to a reduction of $_iH_c$, and it is in agreement with our previous study on $Pr_yFe_{88-y}Ti_2B_{10}$ (y = 7–9.5) nanocomposite ribbons [22]. Furthermore, magnetically amorphous phase appears for y = 7–8, and the amount of amorphous phase is increased with the decrease of Nd content, resulting in the reduction of magnetic properties and the deterioration of SQ, as shown in Fig. 4.

Besides, to optimize the magnetic properties, the effect of B content on the magnetic properties of directly quenched $Nd_{9.5}Fe_{87.5-z}Ti_{2.5}Zr_{0.5}B_z$ (z = 14–19) magnets is also investigated and shown in Fig. 6. It is found that with the increase of B content z, B_r and $(BH)_{max}$ increase from 6.5 kG and 7.8 MGOe for z = 14 to 6.6 kG and 8.2 MGOe for z = 15 at first, and then decrease to 4.0 kG and 2.1 MGOe for z = 19. On the other hand, $_iH_c$ increases from 8.3 kOe for z = 14 to 16 kOe for z = 18 and then reduces to 12.5 for z = 19. This suggests that proper B content of 14–16 at%

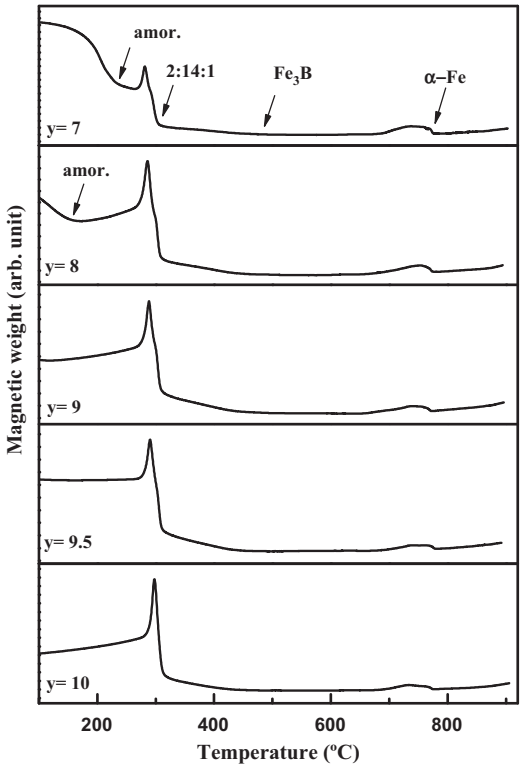

Fig. 5. TMA scans of directly quenched $Nd_yFe_{82-y}Ti_{2.5}Zr_{0.5}B_{15}$ bulk magnets.

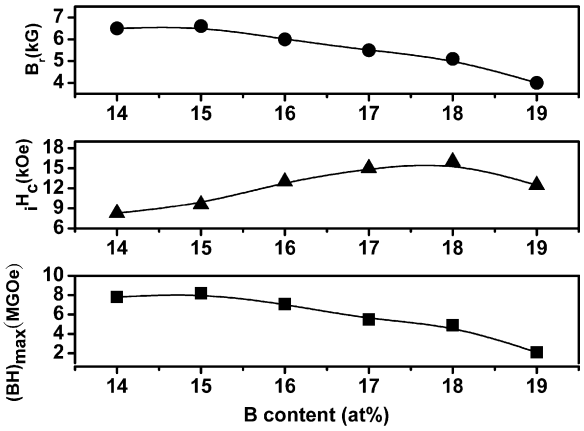

Fig. 6. Magnetic properties variation with B content for directly quenched $Nd_{9.5}Fe_{87.5-z}Ti_{2.5}Zr_{0.5}B_z$ bulk magnets.

is important to obtain the directly quenched rods with both high coercivity of 8.3–13 kOe and energy product of 7.1–8.2 MGOe.

Fig. 7 presents TMA scans of directly quenched $Nd_{9.5}Fe_{87.5-z}Ti_{2.5}Zr_{0.5}B_z$ bulk magnets. It is found that the large volume fraction of magnetically hard 2:14:1 phase coexists with minor amounts of soft Fe_3B and α-Fe phase for $z = 14$–19, and the amorphous phase appears for higher B contents of 18–19 at.%. With the increase of nonmagnetic B content, magnetization of the magnets is diluted, resulting in the reduction of remanence.

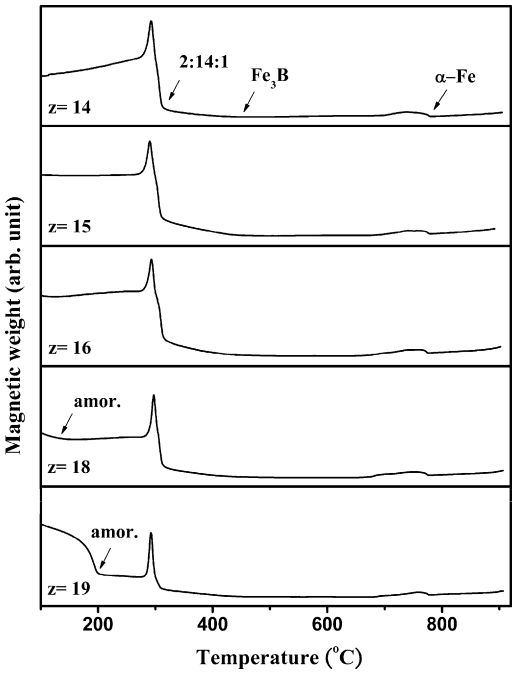

Fig. 7. TMA scans of directly quenched $Nd_{9.5}Fe_{87.5-z}Ti_{2.5}Zr_{0.5}B_z$ bulk magnets.

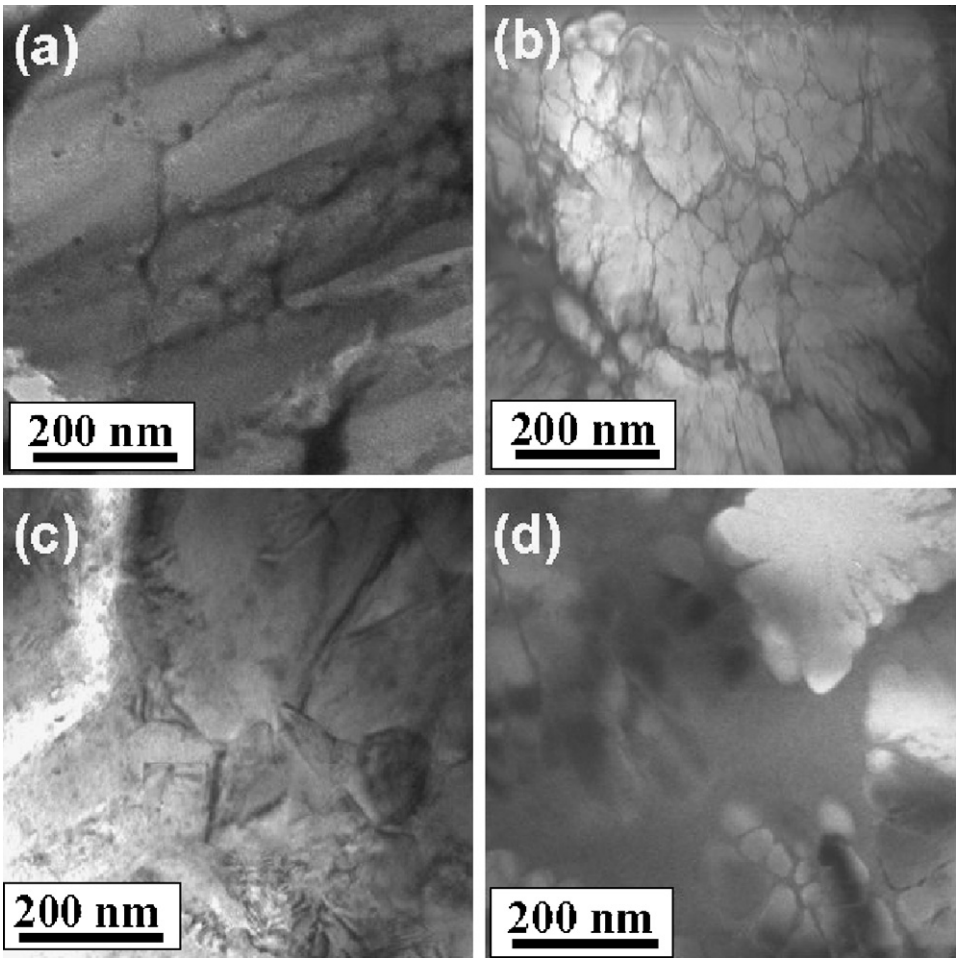

Fig. 8. TEM images of directly quenched (a) Zr-free $Nd_{9.5}Fe_{72.5}Ti_3B_{15}$, (b) $Nd_{9.5}Fe_{72.5}Ti_{2.5}Zr_{0.5}B_{15}$, (c) $Nd_{9.5}Fe_{72.5}Zr_3B_{15}$, and (d) $Nd_{9.5}Fe_{69.5}Ti_{2.5}Zr_{0.5}B_{18}$ bulk magnets.

Table 1
Comparison of the magnetic properties for various RFeB bulk magnets.

Composition	Process route		Size	B_r (kG)	$_iH_c$ (kOe)	$(BH)_{max}$ (MGOe)	Reference
	Precursor	Annealing					
$Nd_{3.1}Dy_{0.5}Fe_{67}Co_{9.4}B_{20}$	Amorphous	640 °C	0.5 mm	11.9	3.1	11.6	[9]
$Pr_{3.5}Fe_{66.5}Co_{10}B_{20}$	Amorphous	590 °C	0.5 mm	12.3	2.8	12.0	[10]
$Pr_3Dy_1Fe_{66}Co_{10}B_{20}$	Amorphous	630 °C	0.5 mm	9.2	3.6	7.3	[12]
$Nd_3Dy_1Fe_{66}Co_{10}B_{20}$	Amorphous	670 °C	0.6 mm	8.6	3.7	9.3	[13]
$Nd_{9.5}Fe_{72.5}Ti_3B_{15}$	As-cast		0.7 mm	6.5	10.3	8.7	[18]
$N_{9.5}Fe_{72.5}Ti_{2.5}Zr_{0.5}B_{15}$	As-cast		0.9 mm	6.6	9.6	8.2	This study

Because the grain size and its distribution of the magnets are very crucial to affect permanent magnetic properties, whereas the grain size nearby the mold is normally fine enough to ensure its high coercivity. Nevertheless, the cooling rate at the core region is lower than that at the peripheral region, and thus, it becomes the major issue to know the microstructure especially at the core region of the magnets. Fig. 8 depicts TEM images of the core region of directly quenched $Nd_{9.5}Fe_{72.5}Ti_3B_{15}$, $Nd_{9.5}Fe_{72.5}Ti_{2.5}Zr_{0.5}B_{15}$, $Nd_{9.5}Fe_{72.5}Zr_3B_{15}$, and $Nd_{9.5}Fe_{69.5}Ti_{2.5}Zr_{0.5}B_{18}$ bulk magnets, respectively. The grain size for the $Nd_{9.5}Fe_{72.5}Ti_3B_{15}$ magnet is estimated to be about 200–250 nm, and it is refined down to 50–100 nm by the substitution of 0.5 at.% Zr for Ti, but as x is increased to 3.0 at.%, the abnormally coarser grains appear, giving rise to the decrease of the magnetic properties. On the other hand, with the increase of B content, the finer grain size is obtained, leading to the increment of intrinsic coercivity.

Besides, a grain boundary phase is observed for these samples. For identifying the composition of the grain and boundary phases for the studied alloys, energy dispersive X-ray analysis (EDX) is employed. The EDX results show that Ti atoms tend to appear at the grain boundaries. It is presumed that Ti prefers to react with the boron in excess to form Ti-boride in the grain boundary, due to the strong affinity between Ti and B. The isolation effect of non-magnetic grain boundary phase is very beneficial in obtaining the magnets with high coercivity [23]. On the other hand, Zr atoms are averagely distributed in both the grain interior and the grain boundary phase. The entrance of Zr element into $Nd_2Fe_{14}B$ unit cell may slightly decrease T_C of 2:14:1 phase, and increase the anisotropy field of the alloy, resulting in the improvement of the coercivity and the magnetic energy product of the bulk magnets. Therefore, the main reasons for the good magnetic properties achieved in these studied alloy rods include the proper volume fraction of magnetically soft and hard phases (2:14:1, Fe_3B, and α-Fe), fine grains, and grain boundary phase due to proper Zr substitution for Ti as well as the appropriate Nd and B contents.

Finally, the magnetic properties of the bulk R–Fe–B magnets developed by other groups previously as well as by our group in the present study are compared and summarized in Table 1. In the case of the magnets made by amorphous precursors followed by annealing, in order to obtain the amorphous phase, high B contents (≧20 at.%) and lower R contents of 3–4 at.% are required to produce bulk magnets with the diameters of 0.5–0.6 mm. After proper annealing at 590–670 °C, 2:14:1 phase is found to coexist with the considerable amount of magnetically soft phases α-Fe and Fe_3B, leading to lower $_iH_c$ of 2.8–3.7 kOe, though larger energy products ($(BH)_{max}$) of 7.3–12.0 MGOe can be obtained.

On the other hand, in our studies, in order to produce the directly casted R–Fe–B bulk magnets, proper high B content of 14–16 at.% is necessary to keep the finer microstructure in the magnet, and the designated R content of 8–10 at.% provides the formation of large amount of 2:14:1 phase. In the meantime, the co-substitution of Ti and Zr can not only well modify magnetic phases constitution but also refine the microstructure effectively. Consequently, the attractive magnetic properties of B_r = 6.0–6.6 kG, $_iH_c$ = 6.7–13.5 kOe and $(BH)_{max}$ = 6.7–8.2 MGOe are attained for $Nd_yFe_{97-y-z}Ti_{3-x}Zr_xB_z$ (x = 0.5–2; y = 8–10; z = 14–16) alloys with the diameters of 0.9 mm. Their magnetic properties are superior to those of the magnets obtained by annealing the amorphous bulk precursors, especially for the $_iH_c$. Besides, proper Zr substitution for Ti does increase the size of the $Nd_{9.5}Fe_{72.5}Ti_3B_{15}$ rod alloy and preserves the attractive magnetic properties.

4. Conclusions

The magnetic properties of directly quenched $Nd_yFe_{97-y-z}Ti_{3-x}Zr_xB_z$ (x = 0–3; y = 7–10; z = 14–19) bulk magnets with a diameter of 0.9 mm are dominated by phase constitution and microstructure. For the alloys with a proper amount of Zr substituting (0.5–2 at.%) Ti, not only the grain refinement but also the Zr element entering into the 2:14:1 phase play an important role in improving the coercivity and the magnetic energy product. As Zr content increases to 3.0 at.%, the significant decrease of the volume fraction of 2:14:1 phase accompanies the appearance of abnormally coarser grains and leads to the decrease of magnetic properties drastically. Besides, proper Nd and B concentrations can well modify the phase constitution. As a result, the magnetic properties of bulk magnetic rods are improved. In this study, the attractive magnetic properties of B_r = 6.0–6.6 kG, $_iH_c$ = 6.7–13.5 kOe and $(BH)_{max}$ = 6.7–8.2 MGOe are achieved for Zr-substituted $Nd_yFe_{97-y-z}Ti_{3-x}Zr_xB_z$ (x = 0.5–2; y = 8–10; z = 14–16) alloys. The good magnetic properties might be the result of proper phases constitution, fine grains, and grain boundary phase.

Acknowledgements

This paper was supported by National Science Council, Taiwan under grant nos. NSC-98-2112-M-194-005-MY3 and NSC-98-2112-M-029-001-MY3.

References

[1] R. Coehoorn, D.B. DeMooij, C. DeWaard, J. Magn. Magn. Mater. 80 (1989) 101.
[2] A. Manaf, R.A. Buckley, H.A. Davis, M. Leonowicz, J. Magn. Magn. Mater. 101 (1991) 360.
[3] E.F. Kneller, R. Hawig, IEEE Trans. Magn. 27 (1991) 3588.
[4] H. Kanekiyo, M. Uehara, S. Hirosawa, IEEE Trans. Magn. 29 (1993) 2863.
[5] J. Bauer, M. Seeger, A. Zern, H. Kronmüller, J. Appl. Phys. 80 (1996) 1667.
[6] K. Raviprsad, M. Funakoshi, M. Umemoto, J. Appl. Phys. 83 (1998) 921.
[7] W.C. Chang, D.Y. Chiou, S.H. Wu, B.M. Ma, C.O. Bounds, Appl. Phys. Lett. 72 (1998) 121.
[8] W.C. Chang, S.H. Wu, B.M. Ma, C.O. Bounds, S.Y. Yao, J. Appl. Phys. 83 (1998) 2147.
[9] W. Zhang, A. Inoue, Appl. Phys. Lett. 80 (2002) 1610.
[10] W. Zhang, A. Inoue, J. Appl. Phys. 91 (2002) 8834.
[11] P. Pawlik, H.A. Davies, Scr. Mater. 49 (2003) 755.
[12] M. Marinescu, P.C. Pawlik, H.A. Davies, H. Chiriac, J. Optoelectron. Adv. Mater. 6 (2004) 603.
[13] M. Marinescu, H. Chiriac, M. Grigoras, J. Magn. Magn. Mater. 290 (2005) 1267.
[14] J. Zhang, K.Y. Kim, Y.P. Feng, Y. Li, Scr. Mater. 56 (2007) 943.

[15] X. Tan, H. Xu, Q. Bai, Y. Dong, Appl. Phys. Lett. 91 (2007) 252501.
[16] H.W. Chang, M.F. Shih, C.W. Chang, C.C. Hsieh, Y.T. Cheng, W.C. Chang, Y.D. Yao, A.C. Sun, Scr. Mater. 59 (2008) 227.
[17] H.W. Chang, M.F. Shih, C.C. Hsieh, W.C. Chang, J. Alloys Compd. 484 (2009) 143.
[18] H.W. Chang, M.F. Shih, C.C. Hsieh, W.C. Chang, J. Alloys Compd. 489 (2010) 499.
[19] Y. Long, W. Zhang, X. Wang, A. Inoue, J. Appl. Phys. 91 (2002) 5227.
[20] Z. Chen, B.R. Smith, D.N. Brown, B.M. Ma, J. Appl. Phys. 91 (2002) 8168.
[21] M. Jurczyk, W.E. Wallace, J. Magn. Magn. Mater. 59 (1986) L182.
[22] H.W. Chang, C.H. Chiu, C.W. Chang, W.C. Chang, A.C. Sun, Y.D. Yao, Scr. Mater. 55 (2006) 529.
[23] E. Girt, K.M. Krishnan, G. Thomas, Z. Altounian, Appl. Phys. Lett. 76 (2000) 1746.